# Seismic Vulnerability of Residential Buildings in Jordan and its Locality

**H. S. Al-Nimry**
*Jordan University of Science and Technology, Jordan*

**SUMMARY:**
This article presents an experimental and analytical investigation of the seismic vulnerability of residential buildings in Jordan that utilize limestone masonry backed with plain concrete in their exterior walls. Two structural systems, associated with the method of construction of exterior walls, namely: bearing walls and RC infilled frame systems were investigated. Five infilled frame specimens and two bearing wall specimens were constructed at one-third scale. Effects of openings, dowels and level of axial loading were examined using quasi-static experimentation. Test results were used to model the effect of stone-concrete walls on the seismic performance of two and four story representative buildings. Pushover analysis was used to arrive at the capacity curves of two dimensional models of the buildings. Five damage states were considered: none, slight, moderate, extensive and complete and damage state thresholds were assigned based on the capacity curves. Fragility curves were developed using the lognormal probability density function.

*Keywords: Bearing walls, infilled frames, quasi-static, pushover analysis, vulnerability functions.*

## 1. INTRODUCTION

The most common type of residential construction in Jordan and its locality utilizes thin limestone masonry units backed with plain concrete (stone-concrete walls) to constitute the perimetric exterior walls. Typically, the walls are constructed using two different methods resulting in two distinct structural systems.

The first system consists of stone-concrete bearing walls complying with the provisions of Jordanian National Building Code for Loads and Forces (JCLF, 1985) and reflecting dominant residential construction in Jordan before the nineties. In this system, the exterior walls consist of stone masonry back-filled with plain concrete and confined with reinforcing columns at their ends and tie beams at the story level. The backing concrete and the confining columns are cast in several horizontal layers with a time gap that could reach several days. The second system represents the current construction practice in Jordan wherein gravity load-designed RC frames are infilled with stone-concrete panels. The latter infill panels comprise a layer of stone masonry back-filled with plain concrete and separated from a second layer of concrete masonry/blocks by thin polystyrene insulating boards. The most prominent feature in these walls is that the back filling concrete is cast in horizontal layers to avoid toppling of the thin stone masonry units. Concurrence of the horizontal bed joints between the stone masonry courses and the resulting construction joints between the different plain concrete layers is avoided.

Few studies provided basic, yet very modest, information on the seismic response of stone-concrete walls (Al-Nimry, 2002; Al-Nimry et al., 2003; Abdel-Halim and Barakat, 2003). This experimental program was devised to further investigate the behavior of such walls under simulated earthquake loading. Seven specimens (two bearing wall models and five infilled frame models) were tested using reversed cyclic loading. The test results were used to develop analytical vulnerability functions for two and four story residential buildings of the two structural systems described above.

## 2. TEST SPECIMENS

### 2.1. General

The test program included two bearing wall models and five single-story, single-bay RC frames. In view of the limited local availability of small size deformed bar reinforcement and the load capacity of the available testing facilities at Jordan University of Science and Technology, prototype subassemblies were modeled at a direct geometrical scale of one-third. Both geometry and reinforcement of the test specimens were determined using standard similitude requirements of practical true models (Harris and Sabnis, 1999). Specimen's designations and test parameters are summarized in Table 2.1.

**Table 2.1** Test Specimens

| Specimen | Description | Opening | Axial Load |
|---|---|---|---|
| BW3 | Bearing Wall | With | Uniformly distributed on tie beam (38 kN) |
| BW4 | Bearing Wall | With | Uniformly distributed on tie beam (65 kN) |
| IF1 | Infilled Frame | With | Two equal concentrated loads (35 kN each) applied to the columns |
| IF2 | Infilled Frame-dowels at base, and at column-infill interface | With | |
| IF3 | Infilled Frame-dowels at base | With | |
| IF5 | Infilled Frame | Without | 50 kN per column |
| IF6 | Infilled Frame | Without | 35 kN per column |

### 2.2. Bearing Wall Models

Two identical bearing wall specimens (BW3 and BW4) comprising a window opening were constructed using the cross-sectional details shown in Figure 2.1(a).

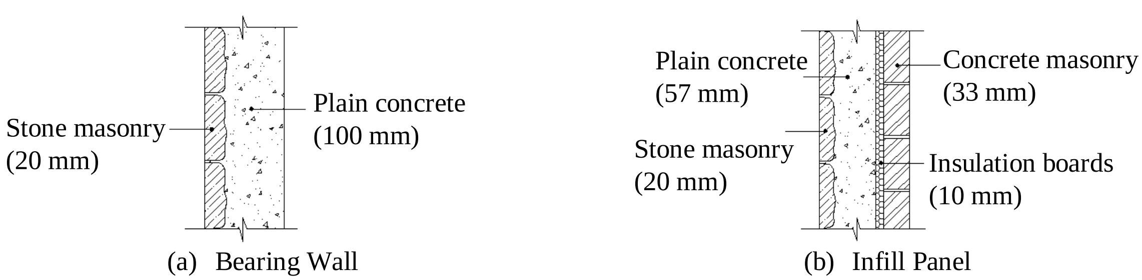


**Figure 2.1** Cross-sectional details of stone-concrete walls

The bearing wall models were confined with reinforcing columns at their ends (boundary elements) and tie beams at the story level as displayed in Figure 2.2. Specimen's layout and reinforcement details, as partially dictated by provisions of the 1985 Jordanian National Building Code (JC, 1985) and the limited availability of small deformed bar sizes are shown in Figure 2.4.

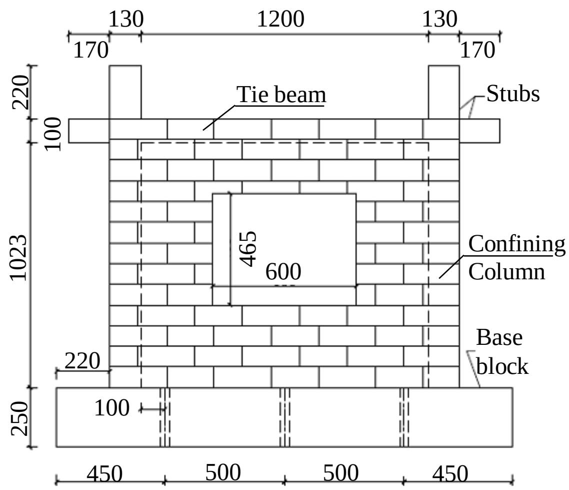


**Figure 2.2** General layout of bearing walls

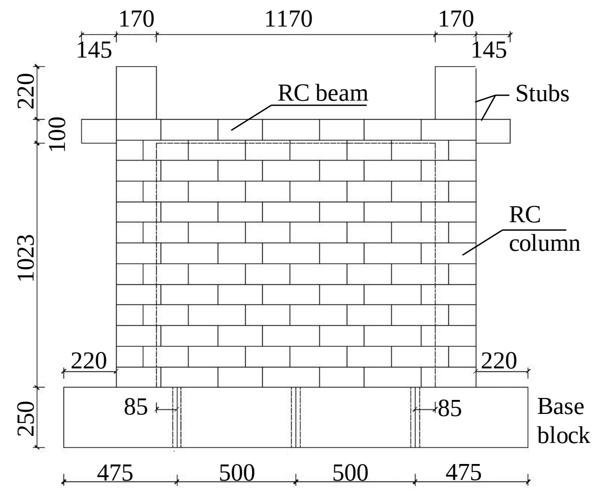


**Figure 2.3** General layout of infilled frames (IF5 and IF6)

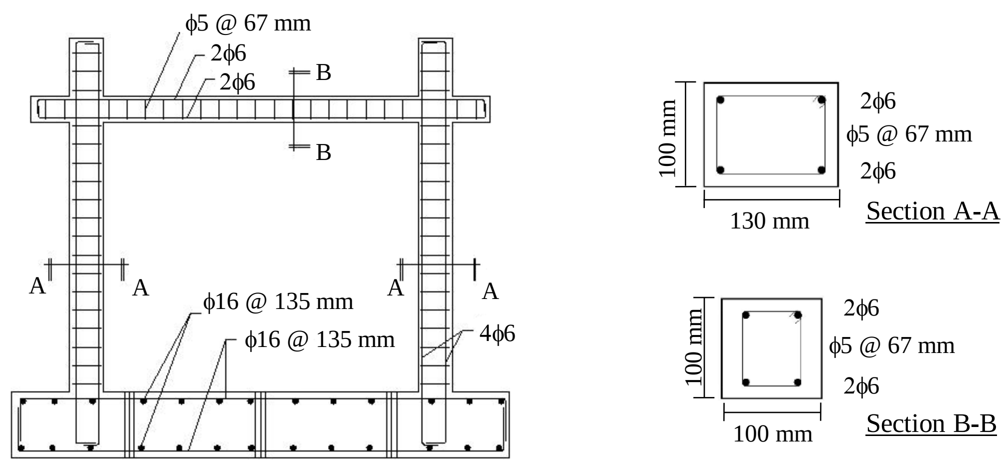


**Figure 2.4** Reinforcement details of bearing walls BW3 and BW4

### 2.3. Infilled Frame Models

Three specimens were included in the study to assess the effect of stone-concrete infill panels with and without window openings on the seismic response of gravity load-designed RC frames: Specimen IF1 comprised a window opening whereas the two identical specimens IF5 and IF6 were constructed without openings. Two infilled frame specimens with a window opening (IF2 and IF3) were devised in accordance with the recommendations of the Jordanian Code for Earthquake Resistant Buildings (JC, 2005) which suggests the use of dowel rebars between the infill panel and the bounding frame elements in areas of low and moderate seismicity. Specimen IF2 incorporated dowel reinforcement at interfaces between the wall, the base block and the bounding columns whereas specimen IF3 had dowel reinforcement only at the interface between the wall and the base block. Cross-sectional details of the infill wall as modeled in test specimens IF1-IF6 are shown in Figure 2.1(b). Concrete masonry used in the models was also scaled from prototype concrete blocks (100x200x400 mm) at one-third scale. The bed and head mortar joints between the different masonry units, both stone and concrete, were kept around 5-mm thick.  General layout and reinforcement details of the RC frame specimens IF1-IF6 are shown in Figures 2.3 and 2.5, respectively.

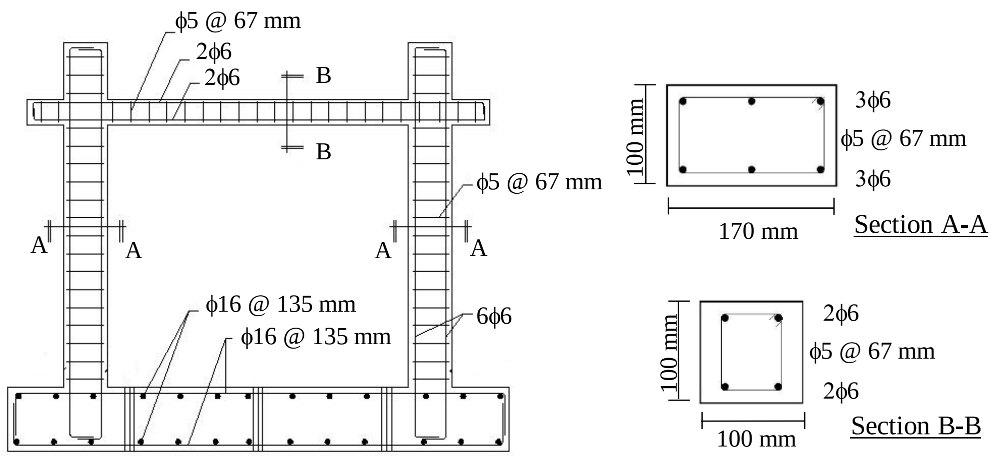


**Figure 2.5** Reinforcement details of infilled frame specimens (IF1-IF6)

## 2.4. Material Properties

The 10 mm maximum aggregate size of the model concrete was determined based on ACI Code requirements (ACI, 2005) in conformity with cover and reinforcement spacing rather than scaling it down from that of the prototype concrete. Three different concrete mixes were designed to produce the target compressive strength $f'_c$ as measured on 150x300 mm cylinders: for the RC columns of the infilled frames; for the RC beams in all specimens; and for the back-filling plain concrete of the infill panels and the bearing wall specimens. No special measures were taken to model the tensile strength of prototype concrete. Table 2.2 summarizes compressive strength results of the used concretes.

**Table 2.2** Average Compressive Strength Results of the Model Concretes

| Specimen Designation | Compressive Cylinder Strength (MPa) at 28-days | | |
|---|---|---|---|
| | Beams | Columns | Infill Panel |
| BW3 and BW4 | 29.5 | 18.0 | Not applicable |
| IF5-IF6 | 32.5 | 20.6 | 16.6 |

Deformed bars of 6 mm and 5 mm diameter were provided through a local producer of cold drawn steel mesh. Based on nominal bar diameters, yield and ultimate tensile strengths of the main model reinforcement were determined at 472 MPa and 512 MPa, respectively with a 9.3% elongation at failure. Compressive strength of the limestone masonry was 65 MPa determined in accordance with ASTM-C170 specification. Scaled limestone stone masonry units were used. Concrete masonry units 33x67x135 mm were scaled directly from the 100x200x400 mm prototype masonry using a 1/3 scale and an average 7-day compressive strength of 4.6 MPa. A mix of 1:0.5:4 (cement: lime: aggregates) proportion by volume was used to prepare cement mortar with an average 28-day compressive strength of 11.8 MPa.

## 3. TEST SETUP AND LOADING PROGRAM

To simplify the interpretation of results in terms of ductility and to enable continued testing past the peak load-carrying capacity of the tested model; the test specimens were subjected to a constant axial load and to a displacement-controlled reversed cyclic lateral load. Lateral loading was applied to the test specimens through a displacement-controlled hydraulic actuator with a load capacity of 417 kN in compression and 254 kN in tension with a 300 mm stroke. Axial loads were applied to the two columns of the infilled frames using two hydraulic actuators each with a load capacity of 163 kN in compression. To test the bearing walls, three rollers resting on top of a stiff steel distributing beam were arranged to accommodate the expected story drift and minimize the frictional resistance as shown in Figure 3.1.

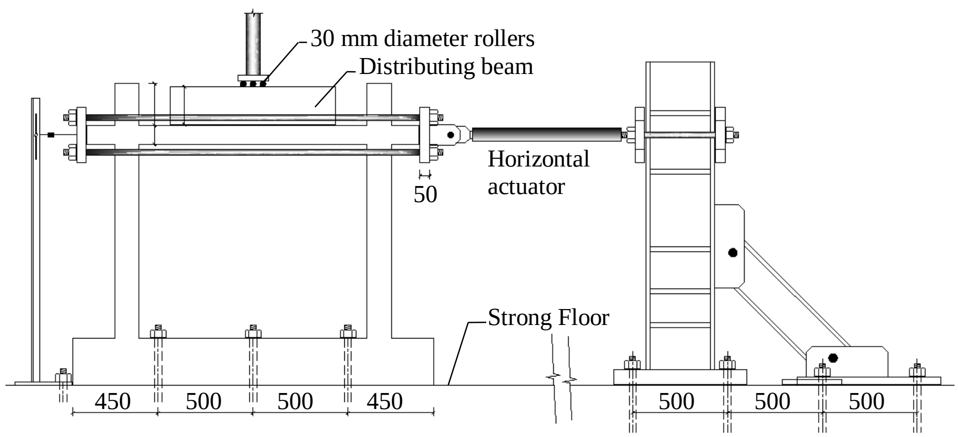


**Figure 3.1** Test setup

The target axial load was first applied to the test specimen and maintained constant to the end of the test program. The test specimens were subjected to a number of elastic cycles followed by sets of constant amplitude cycles at the first yield displacement ($\Delta_{y1}$) and at multiples of this displacement until failure occurred. An example of the adopted displacement histories is presented in Figure 3.2.

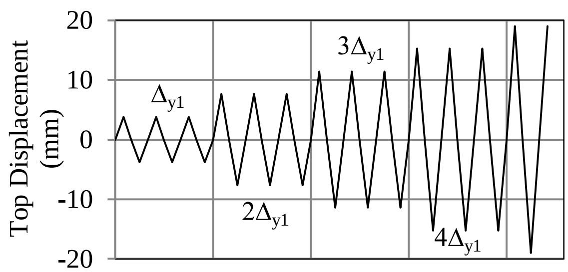


**Figure 3.2** Top displacement history for specimen BW4

## 4. EXPERIMENTAL RESULTS

The experimental hysteresis loops of the two bearing wall specimens and the accompanying hysteresis envelopes, displayed in Figures 4.1-4.2, relate the top displacement to the restoring force as measured under reversed cyclic loading including the pre-yield stage.

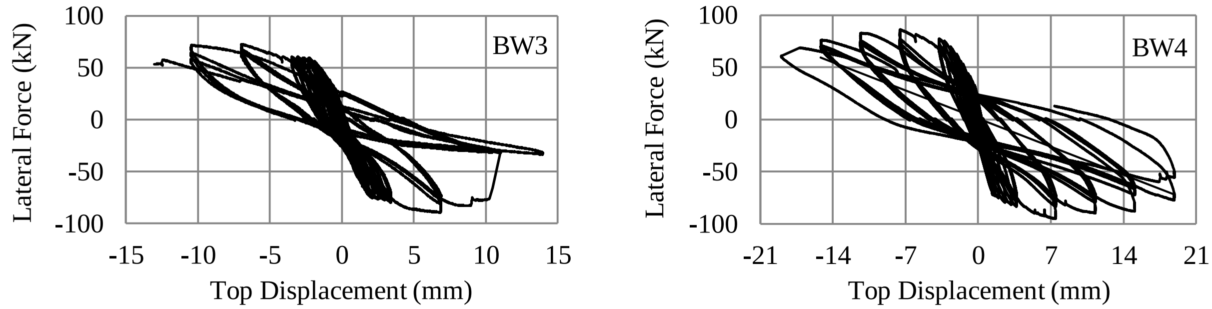


**Figure 4.1** Restoring force-top displacement hysteresis loops for the two bearing wall specimens

The hysteresis envelopes of the two bearing wall models (Figure 4.2) display the beneficial effect of axial load on the lateral strength and ductility of the test specimens. The lateral resistance of specimen BW4 increased by 11% over that of BW3 whilst the secant stiffness at first yield increased by 7% only. The effect of axial loads was more pronounced in the case of solid walls (without a window opening) resulting in substantial increases in both lateral strength and stiffness of the walls (Al-Nimry 2002).

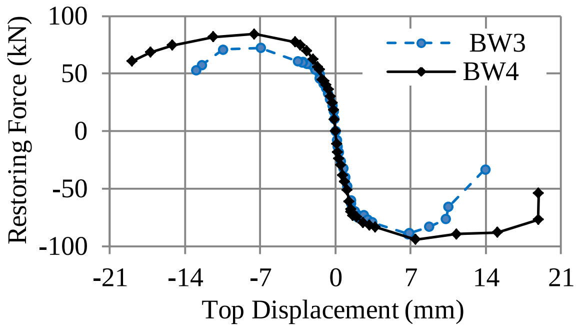


**Figure 4.2** Hysteresis envelopes-bearing wall specimens

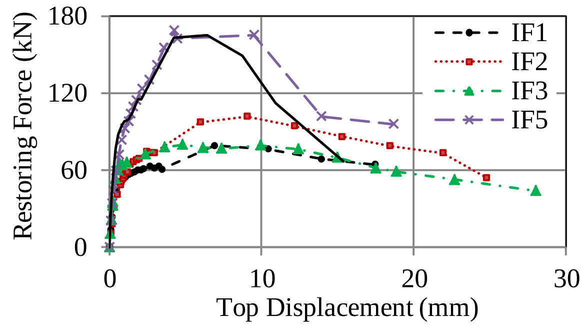


**Figure 4.4** Average restoring force-top displacement hysteresis envelopes for infilled frame specimens

Figure 4.3 deploys a sample of the experimental hysteretic behavior obtained for the infilled frames. The average hysteresis envelopes of the infilled frame models, presented in Figure 4.4, indicate that solid infilled frame models (IF5 and IF6) have 1.6-2.1 times the maximum lateral resistance of frame models bounding an infill with a central opening.

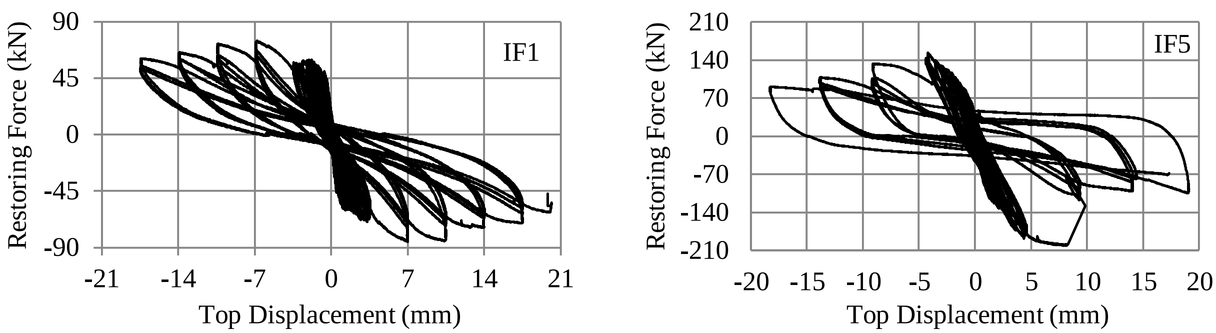


**Figure 4.3** Restoring force-top displacement hysteresis loops for infilled frame specimens IF1 and IF5

Full details of the experimental program are available in Al-Nimry (2010). However, the following points summarize some of the test results:

- Using dowels at the infill interface with the base block, as in specimen IF3, enhanced the ductility of the frame-infill system by about 26% without affecting its maximum load-carrying capacity.
- Infilled frame model IF2 with dowel rebars at the infill interface with the base block and the two bounding columns was capable of withstanding almost 1.29 times the load-carrying capacity of specimen IF1 without dowels. The two specimens attained a global displacement ductility of about 5.
- Compared with IF6, wherein the infill panel has no windows, lateral resistance of specimen IF1 with the window opening dropped by 52% and its initial secant stiffness by 38%. Both specimens lost 20% of their maximum lateral resistance at a global ductility ratio of about 5.
- Minor increase in the lateral resistance of specimen IF5 (about 2%) was detected as a result of higher axial loads compared to the companion specimen IF6. However, the global displacement ductility of specimen IF5 was about half that of specimen IF6.

# 5. ANALYTICAL MODELING

## 5.1. Macro-Modeling of Stone-Concrete Walls

Using SAP2000N v14.1 (Computers and Structures, 2009), simple analytical models were built to represent the lateral resistance and stiffness observed during quasi-static testing of bearing wall specimens BW3 and BW4, infilled frame specimen IF1 (comprising a window opening) and specimens IF5 and IF6 (without openings). Based on the damage imparted to test specimens BW3 and BW4 under reversals of lateral loading, two wall piers (with a width equal to the distance between the inner edge of the reinforcing columns and the window opening) were defined and assigned a roller support at the base as the body of the wall was free to slide over the base block. The tie beam extending between the two reinforcing columns was also connected to the wall piers as shown in Figure 5.1. The reinforcing columns were fixed at the base and coupled P-M3 hinges were assigned at their ends.


**Figure 5.1** SAP2000 model for specimens BW3 and IF1

The nonlinear response of the wall was modeled using a nonlinear link element which was assigned a multi-linear plasticity property with nonlinear behavior for the axial direction only. The force displacement relation governing its hysteretic behavior was calibrated to conform to experimental data. Similarly, effect of the infill panel (strut action) on the lateral resistance of the bounding frame in specimens IF1, IF5 and IF6 was modeled using a diagonal nonlinear link element, as shown in Figure 5.1.

The link element was assigned a multi-linear plastic property with nonlinear behavior for the axial direction characterized by a force displacement relation calibrated to conform to experimental data. P-M3 hinges were introduced at the end sections of the two bounding columns. No hinges were assigned to the beam to replicate test results wherein steel strain measurements did not indicate any yielding in the beam section. Nonlinear static analysis was performed to simulate the quasi-static tests of the different specimens. The analytical pushover curves for BW3 and IF1displayed in Figures 5.2 and 5.3, respectively exhibit good agreement with the experimental restoring force-top displacement relations.

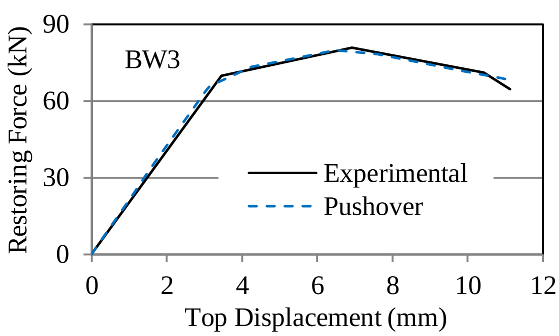


**Figure 5.2** Pushover curve for specimen BW3

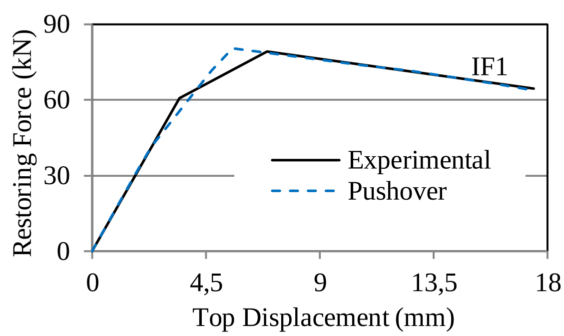


**Figure 5.3** Pushover curve for specimen IF1

### 5.2. Full Scale Models

The soil at the construction site was assumed to be rock; class $S_B$ with shear wave velocities of about 750 m/sec. All wall panels were assumed to have a central window opening with the ratio between the opening area and the wall similar to that used in the test specimens.

*5.2.1. Bearing wall construction prior 1985 (Type 1 construction, T1)*

Two story (T1LR) and four story (T1MR) regular buildings with exterior stone-concrete walls representative of those dominant in Jordan before 1985 were investigated. Based on estimations of the relative stiffness of interior columns and partitions, stiffness of the exterior bearing wall in each direction was set equal to one-third the building stiffness in that direction. Two dimensional models of the exterior bearing walls extending in the two principal directions of the representative buildings were established using SAP2000 and utilizing the macro models obtained earlier for specimens BW3 and BW4. User-defined P-M3 hinges were introduced in all reinforcing columns at their end sections. The nonlinear link elements were assigned a multi-linear plasticity property with nonlinear behavior in the axial direction only. Nonlinear link elements used in the bottom two stories were assigned a force displacement relation scaled up from that used in BW4 whereas nonlinear link elements used in the upper two stories were based on specimen BW3.

*5.2.2. Infilled frame construction post 1985 (Type 2 construction, T2)*

Two story (T2LR) and four story (T2MR) regular buildings representing the construction practice in Jordan post 1985 were built using results from pushover analyses of the relevant test specimens. Out-of-plane failure of the infill panels was neglected. Based on stiffness computations of interior frames with concrete masonry infills (100 mm thick), stiffness of the exterior infilled frame in each principal direction was set equal to one-third the building stiffness in that direction. Two dimensional models of the exterior RC frames extending along the two principal directions of the representative buildings were built using SAP2000 and utilizing the macro models developed earlier for specimen IF1.User defined P-M3 hinges were introduced in all columns at their end sections.

### 5.3. Capacity Curves

Nonlinear static analysis was used to arrive at the capacity curves of the 2D exterior walls and infilled frames of the representative buildings. Following ATC-40 (1996) recommendations, lateral forces were applied at the different story levels using an inverted triangular lateral loading pattern in proportion to the standard code procedure. The lateral loads applied to each of the exterior walls (whether of the bearing wall or of the infilled frame type) represented one-third the base shear in that direction. Masses assigned to the structural models were applied with the same proportion. For the gravity load case, 50% of the live loads were considered in addition to dead loads. The resulting capacity curves in the two principal directions of analysis were reduced by 25% to account for the various uncertainties regarding the actual seismic response of the buildings considered and uncertainties associated with the analytical modeling.

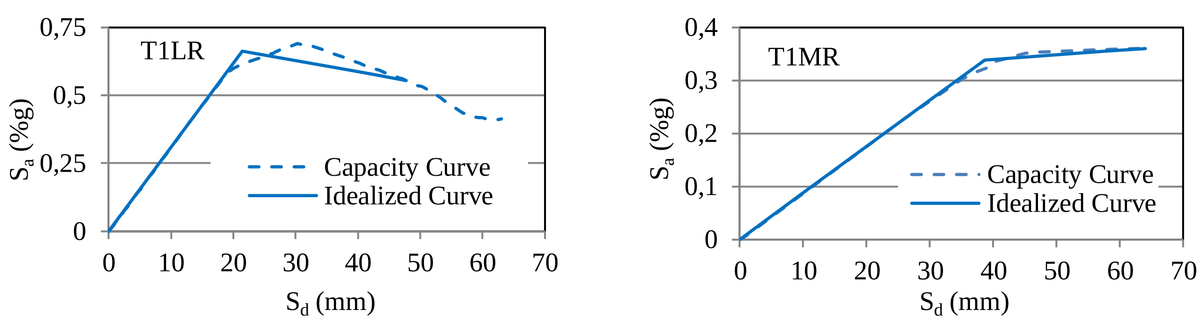


**Figure 5.4** Capacity curves for two story and four story buildings of Type 1 construction

The final capacity curve for a specific building represents the simple mean of the two reduced component capacity curves. Figures 5.4 and 5.5 present the actual and idealized (bilinear format) capacity curves for bearing wall construction (T1LR and T1MR) and infilled frames (T2LR and T2MR), respectively.

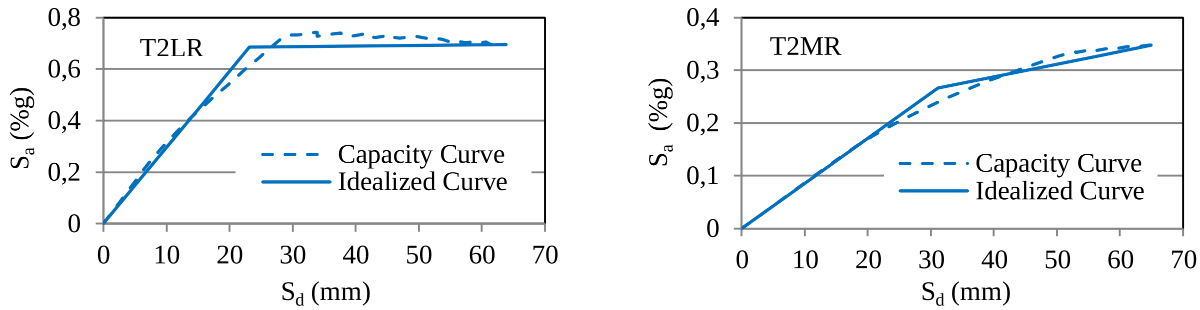


**Figure 5.5** Capacity curves for two story and four story buildings of Type 2 construction

## 6. FRAGILITY CURVES

Fragility curves are plots of the probability of being in a specific damage state P(d≥ds) versus the spectral displacement $S_d$ which defines level of seismic action affecting the structure. For a given damage state, a fragility curve is well described by the lognormal probability density function given in Eqn 6.1:

$$P[ds|S_d] = \Phi\left[\frac{1}{\beta_{ds}} ln\left(\frac{S_d}{S_{d,ds}}\right)\right] \tag{6.1}$$

where $S_{d,ds}$ is the median value of spectral displacement at which the building reaches the threshold of the damage state, ds; $\beta_{ds}$ is the standard deviation of the natural logarithm of spectral displacement of damage state, ds; $\Phi$ is the standard normal cumulative distribution function; and $S_d$ is the spectral displacement.
In this study five damage states are considered: none, slight, moderate, extensive and complete and are assigned the numbers 0, 1, 2, 3 and 4, respectively. Using the idealized capacity curves, values for the damage state thresholds $S_{d,ds}$ are related to the yield and ultimate spectral displacements as follows:

| | | |
|---|---|---|
| None: | $Sd_0 = 0.25Sd_y$ | |
| Slight: | $Sd_1 = 0.70\ Sd_y$ | |
| Moderate: | $Sd_2 = Sd_y$ | (6.2) |
| Extensive: | $Sd_3 = Sd_y+0.75(Sd_u-Sd_y)$ | |
| Complete: | $Sd_4 = Sd_u$ | |

Lognormal standard deviation ($\beta_{ds}$) values that describe the variability of fragility curves for each of the damage states are based on suggested values by FEMA (2003). Assuming moderate variability of the capacity curves ($\beta_c = 0.3$), major post yield degradation ($\kappa = 0.5$), small damage variability ($\beta_{T,ds} = 0.2$) for none, slight and moderate damage and moderate damage variability ($\beta_{T,ds} = 0.4$) for extensive and complete damage the Beta values are obtained for low rise and medium rise buildings. According to Eqn. 6.1, fragility curves follow the lognormal probability distribution and hence can be defined using the mean spectral displacement $S_{d,ds}$ and the corresponding standard deviation $\beta_{ds}$. Fragility curves are presented in Figure 6.1 for the two story and four story buildings representative of dominant Jordanian residential construction before 1985 (T1LR and T1MR) and for two and four story RC skeletons infilled with stone-concrete walls of the type used post 1985 (T2LR and T2MR).

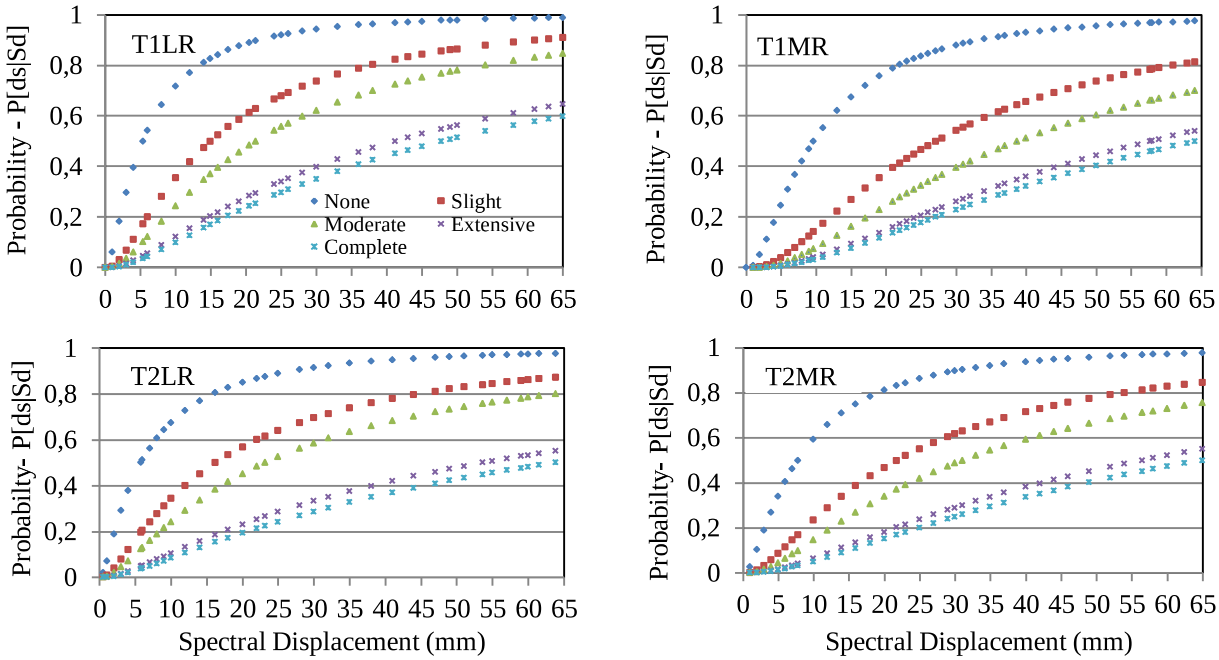


**Figure 6.1** Fragility curves for two and four story buildings representative of residential construction in Jordan

**ACKNOWLEDGMENTS**

The work presented in this paper was funded by the Swiss Agency for Development and Cooperation and implemented under agreement No. 26/2007 with the Building Research Centre of the Royal Scientific Society. The experimental program of the study was conducted at Jordan University for Science and Technology. The support of the technical staff at the Building Research Center of the Royal Scientific Society is acknowledged.

**REFERENCES**

Abdel-Halim, M. and Barakat, S. (2003). Cyclic Performance of Concrete-Backed Stone Masonry Walls. *Journal of Structural Engineering, ASCE*. **129:5**, pp. 596-605.

Al-Nimry, H. (2002). Seismic Response of Stone-Concrete Bearing Walls and Infilled Frames. Ph.D. Dissertation, University of Jordan, Jordan.

Al-Nimry, H.S., Armouti, N.S. and Najmi, A.S. (2003). Inelastic Cyclic Response of Stone-Concrete Bearing Walls. *Journal of the International Association of Concrete Technology*, **1:2**, pp. 119-132.

Al-Nimry, H. (2010). Evaluation of Seismic Performance of Stone-Concrete Residential Buildings in Jordan. Technical Report, Royal Scientific Society, Amman-Jordan.

American Concrete Institute (2005). Building Code Requirements for Structural Concrete (318M-05) and Commentary (318RM-05), Farmington Hills, Michigan.

ATC (1996). Seismic Evaluation and Retrofit of Concrete Buildings, Report ATC-40. Applied Technology Council, Redwood City, California, U.S.A.

Computers and Structures Inc. (2009). SAP2000N v14.1 Reference Manual. Berkeley, U.S.A.

FEMA (2003). HAZUS-MH Technical Manual, Federal Emergency Management Agency,.Washington, DC, U.S.A.

Giovinazzi, S. (2005). The Vulnerability Assessment and the Damage Scenario in Seismic Risk Analysis. Dissertation. Technical University Carolo-Wilhelmina at Braunschweig and University of Florence.

Harris, H.G. and Sabnis, G.M. (1999). Structural Modeling and Experimental Techniques, 2nd edition. CRC Press LLC. U.S.A.

Jordanian National Building Council, JC (1985). Jordanian National Building Code for Loads and Forces, Jordan.

Jordanian National Building Council, JC (2005). Jordanian National Building Code for Earthquake-Resistant Buildings, Jordan.